Gap-bridging enhancement of modified Urca processes in nuclear matter

Mark G. Alford and Kamal Pangeni
Physics Department, Washington University, St. Louis, Missouri 63130, USA
(Received 16 November 2016; published 11 January 2017)

In nuclear matter at neutron-star densities and temperatures, Cooper pairing leads to the formation of a gap in the nucleon excitation spectra resulting in exponentially strong Boltzmann suppression of many transport coefficients. Previous calculations have shown evidence that density oscillations of sufficiently large amplitude can overcome this suppression for flavor-changing β processes, via the mechanism of "gap bridging." We address the simplifications made in that initial work, and show that gap bridging can counteract Boltzmann suppression of neutrino emissivity for the realistic case of modified Urca processes in matter with $^3P_2$ neutron pairing.

DOI: 10.1103/PhysRevC.95.015802

I. INTRODUCTION

Ultra-dense nuclear matter is believed to be a superfluid (via neutron Cooper pairing) and a superconductor (via proton Cooper pairing) for at least part of the range of densities that is relevant for neutron star physics [1–3]. This has a profound effect on transport properties, many of which are suppressed as $\exp(-\Delta/T)$ by the gap Δ in the neutron or proton spectrum. Since neutron star core temperatures T are of order 0.01 MeV [4] and Δ is typically in the MeV range [1], the suppression factor can be as strong as 10^{-40}.

It has previously been shown [5] that compression oscillations of sufficiently high amplitude can entirely overcome this suppression for certain transport properties, such as bulk viscosity and neutrino emissivity, that are dominated by flavor-changing β (weak interaction) processes. The mechanism, called "gap bridging," is a threshold-like behavior, separate from high-amplitude suprathermal enhancement of β processes [6–8]. Additional enhancement may come from the suppression of the gap itself by high-velocity flow of the superfluid relative to the normal fluid [9].

The previous calculation of gap bridging [5] found that oscillations with density amplitude that reached $\Delta n/\bar{n} \sim 10^{-4}$ could show gap-bridging enhancement. Gap bridging is therefore expected to be relevant to high-amplitude oscillations of neutron stars such as *f*- or *r*-modes [10,11], or the oscillations caused by star quakes [12] or neutron star mergers [13]. However, the previous calculation was an illustrative proof of principle in which the neutron pairing was assumed isotropic, in the $^1S_0$ channel, and only direct Urca processes were considered. In this paper we provide a more realistic calculation, obtaining the gap-bridging enhancement of the modified Urca neutrino emissivity for nuclear matter with $^3P_2$ neutron pairing. We find that gap bridging is just as dramatic in this realistic scenario as the original estimates indicated.

In Sec. II we describe the modified Urca process and the quantities that we will calculate to characterize the neutrino emissivity of nuclear matter. In Sec. III we calculate the modified-Urca emissivity for matter with $^1S_0$ pairing of neutrons. In Sec. IV we calculate the modified-Urca emissivity for matter with $^3P_2$ pairing of neutrons. Section V contains our conclusions.

II. MODIFIED URCA PROCESS

Urca processes change the flavor (isospin) of nucleons and emit neutrinos. They dominate certain physical properties such as bulk viscosity and neutrino emissivity. In this paper we will calculate the enhancement of the neutrino emissivity by gap bridging in high-amplitude compression oscillations.

Initial work on gap bridging studied the direct Urca process because of its simplicity, but in β-equilibrated nuclear matter direct Urca processes occur only when the density reaches several times the nuclear saturation density, at which point the proton and neutron Fermi momenta are sufficiently similar to allow direct conversion of one species into the other. In most if not all regions of a neutron star, the direct Urca process $n \to p\, e^-\, \bar{\nu}_e$ is forbidden by energy and momentum conservation: a neutron near its Fermi momentum p_{Fn} cannot turn into a proton near its Fermi momentum p_{Fp} and an electron near its Fermi momentum p_{Fe} because $p_{Fn} > p_{Fp} + p_{Fe}$. In the absence of the direct Urca process, the main flavor-changing β process is the modified Urca process in which a "spectator" neutron, interacting via pion exchange, absorbs the extra momentum (Fig. 1)

$$\begin{aligned} n + n &\to n + p + e^- + \bar{\nu}_e, \\ p + n + e^- &\to n + n + \nu_e. \end{aligned} \tag{1}$$

We neglect the modified Urca process that uses a spectator proton because it is suppressed by the lower density of the protons.

The neutrino emissivity (energy radiation rate per unit volume) arising from the modified Urca process (1) is [14]

$$\epsilon = \int \left[\prod_{j=1}^{4} \frac{d^3P_j}{(2\pi)^3}\right] \frac{d^3P_e}{(2\pi)^3}\frac{d^3P_\nu}{(2\pi)^3}(2\pi)^4\delta(E_{\rm f} - E_{\rm i}) \times \delta^3(\vec{P}_{\rm f} - \vec{P}_{\rm i}) E_\nu f_1 f_2 (1-f_3)(1-f_4)(1-f_e)|M_{\rm fi}|^2, \tag{2}$$

where the index j labels the four nucleon states (two neutrons in the initial state "i" and a proton and a neutron in the final state "f"); $f_j \equiv 1/\{1+\exp[(E_j-\mu_j)/T]\}$ are the Fermi-Dirac occupation distributions for the nucleons, P_j are the nucleon momenta, P_e and E_e are the electron momentum and energy, P_ν and E_ν are the neutrino momentum and energy, and

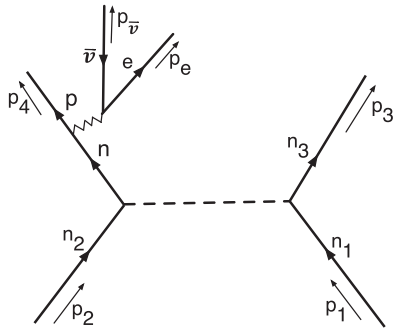

FIG. 1. Feynman diagram for a modified Urca process. The initial state contains two neutrons: n_2, which undergoes β decay to a proton, and n_1, which is a spectator, interacting with the other neutron or proton via the strong nuclear force.

$|M_{\rm fi}|^2$ is the squared matrix element summed over spin states. In superfluid matter the matrix elements acquire coherence prefactors (Bogoliubov coefficients) because the quasiparticles are a superposition of particles and holes. We will neglect these prefactors, which is valid when $\Delta \ll \mu$ [15,16].

The matrix element $|M_{\rm fi}|$ depends on the magnitude and relative orientation of the particle momenta and thus cannot be taken out of the integral. However, because of the strong degeneracy of nucleons and electrons in nuclear matter, the main contribution to the integral in Eq. (2) comes from the region near the Fermi surface. Therefore, we can set $|\vec{p}| = p_F$ in all smooth functions of energy and momenta. Furthermore, in the approximation where we treat the nucleons as nonrelativistic and ignore the neutrino momenta as well as the electron and the proton momenta (which are all small in the region of our interest), the matrix elements turn out to be independent of the relative orientation of the particle momenta [14,17]. This enables us to take the matrix element out of the integral. Since we will be interested in calculating the ratio of the the neutrino emissivity rate with and without superconductivity or superfluidity, the matrix element cancels out at leading order in μ_Δ/p_F expansion. Interested readers can find the expression for the matrix element in Eq. 139 of [14] and Eq. 36 of [17].

A. Effect of superfluidity

We will consider phases of nuclear matter with neutron superfluidity, with or without proton superconductivity. The superfluidity or superconductivity arises from Cooper pairing due to the attractive nuclear force between nucleons. Cooper pairing creates a gap in the energy spectrum of the particles near the Fermi surface. For nuclear matter in neutron stars the temperature is far below the Fermi energy, so only the degrees of freedom close to the Fermi surface are relevant for transport. Their dispersion relation $E_i(p_i)$ is

$$(E_i - \mu_i)^2 = v_{\rm Fi}^2 (p_i - p_{\rm Fi})^2 + \Delta_i^2, \tag{3}$$

where $i = n$ or p indexes the nucleon species, and Δ_i is the gap arising from Cooper pairing. For electrons and neutrinos we can use the free dispersion relations $E_e^2 = p_e^2 + m_e^2$ and $E_\nu = p_\nu$.

We will write the neutrino emissivity ϵ as

$$\epsilon = R_\epsilon\, \epsilon_0, \tag{4}$$

where ϵ_0 is the purely thermal emissivity (with no external compression oscillations) for nonsuperfluid matter, and R_ϵ is the "modification factor" that takes into account the effects of gaps in the fermion spectra and high-amplitude effects such as suprathermal enhancement and gap bridging. As the gap rises, R_ϵ drops below 1 because of Boltzmann suppression [18] but in the presence of compression oscillations that drive the system out of β equilibrium R_ϵ can be pushed up to very large values. The modification function R_ϵ for the modified Urca process is

$$\begin{aligned} R_\epsilon = {} & \frac{945\, P_{Fn}^3}{92104\,\pi^{13}} \int_0^\infty dx_\nu x_\nu^3 \prod_{i=1}^{3} \left[\int_{-\infty}^{\infty} dx_{ni}\, W(x_{ni}, \Delta_n/T) \right] \\ & \times \int_{-\infty}^{\infty} dx_p W(x_p, \Delta_p/T)\; A\; [f(X_-) + f(X_+)] \\ & \times f(x_{n1}) f(x_{n2}) f(-x_{n3}) f(-x_p), \end{aligned} \tag{5}$$

where

$$W(x,z) \equiv \frac{|x|\Theta(x^2 - z^2)}{\sqrt{x^2 - z^2}}, \tag{6}$$

$$\Theta(a) \equiv 1 \text{ if } a > 0, \quad \text{or } 0 \text{ if } a < 0, \tag{7}$$

$$A \equiv 4\pi \int \prod_{j=1}^{5} d\Omega_j \delta^3(\vec{P}_{\rm f} - \vec{P}_{\rm i}), \tag{8}$$

$$X_\pm \equiv x_{n3} + x_p + x_\nu - x_{n1} - x_{n2} \pm \mu_\Delta/T, \tag{9}$$

$$\mu_\Delta \equiv \mu_n - \mu_p - \mu_e, \tag{10}$$

$$f(x) \equiv 1/(1 + e^x), \tag{11}$$

$$x_i \equiv (E_i - \mu_i)/T. \tag{12}$$

The subscripts $n1$ and $n2$ refer to the incoming neutrons; $n3$ and p refer to the outgoing neutron and proton. The chemical potential μ_Δ arises from external compression oscillations that drive the system out of β equilibrium. R_ϵ is normalized so that $R_\epsilon = 1$ when all the gaps are zero and $\mu_\Delta = 0$.

We will calculate $R_{\bar{\epsilon}}$, which measures how much the emissivity is affected by nonlinear high-amplitude effects and by Cooper pairing,

$$\begin{aligned} R_{\bar{\epsilon}}(\hat{\mu}_\Delta) &= \frac{\langle \epsilon(\mu_\Delta) \rangle}{\langle \epsilon_0 \rangle} = \langle R_\epsilon(\mu_\Delta) \rangle, \\ \mu_\Delta(t) &= \hat{\mu}_\Delta \sin(\omega t), \end{aligned} \tag{13}$$

where $\langle X \rangle$ means the average of X over one oscillation cycle. Since ϵ_0, the emissivity in the absence of oscillations and with no Cooper pairing, is independent of μ_Δ, then $\langle \epsilon_0 \rangle = \epsilon_0$.

III. SINGLET STATE ($^1S_0$) PAIRING FOR BOTH NUCLEONS

We first consider modified-Urca neutrino emission in matter where both the neutrons and protons form Cooper pairs in the $^1S_0$ state. As we will see in Sec. IV, the results for the realistic case of $^3P_2$ neutron pairing are qualitatively and quantitatively

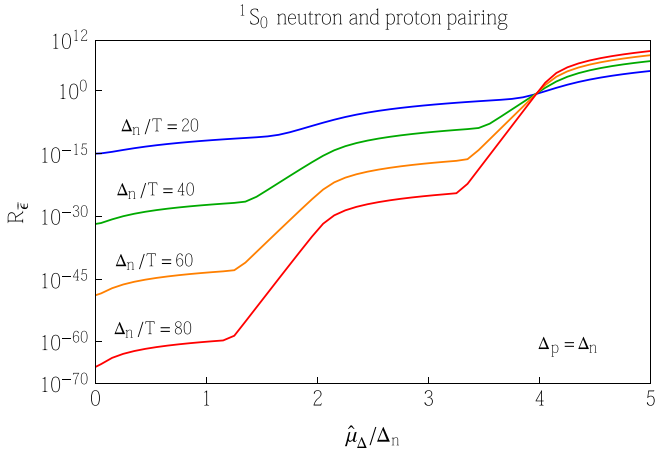

FIG. 2. Dependence of neutrino emissivity [via the averaged modification function $R_{\tilde{\epsilon}}$, Eqs. (13) and (4)] on the amplitude of the applied oscillation [via the departure μ_Δ from β equilibrium, Eq. (10)], for $^1S_0$ neutron and proton pairing. At low amplitude the emissivity is Boltzmann suppressed by the gaps, but for high enough amplitude gap bridging reverses the suppression.

similar to this case. For $^1S_0$ pairing the gap is isotropic so the angular integral A and the radial integral in Eq. (5) can be separated. After angular integration, the modification function is

$$R_\epsilon = \frac{60480}{11513\pi^8}\int_0^\infty dx_\nu x_\nu^3 \prod_{i=1}^{3}\int_{-\infty}^{\infty} dx_{ni}\, W(x_{ni},\Delta_n/T) \times \int_{-\infty}^{\infty} dx_p W(x_p,\Delta_p/T) f(x_{n1}) f(x_{n2}) f(-x_{n3}) f(-x_p) \times [f(X_-) + f(X_+)]. \quad (14)$$

In Fig. 2 we show the effect of increasing the amplitude of the applied compression oscillations for the case where protons and neutrons have the same $^1S_0$ gap, $\Delta_p = \Delta_n$. For low-amplitude oscillations the system remains in β equilibrium ($\hat{\mu}_\Delta/\Delta_n \ll 1$) and the neutrino emissivity is very heavily suppressed by the gaps, roughly as $\exp(-2\Delta_n/T)$. As the amplitude rises, $R_{\tilde{\epsilon}}$ rises due to suprathermal effects [a factor of $(\mu_\Delta/T)^8$ [7]]. On the log scale used in Fig. 2 this appears as a very slow, logarithmic, increase. When $\hat{\mu}_\Delta$ becomes of the same order as Δ_n, gap bridging begins to occur: some β processes start to become unsuppressed, and their rate rises exponentially (straight line on this plot). As we discuss in more detail below, this happens in two steps, until at high amplitude of the oscillations, $\hat{\mu}_\Delta/\Delta_n \approx 4$, all the Boltzmann suppression due to the gap has been overcome, and $R_{\tilde{\epsilon}} \approx 1$, regardless of how low the temperature may be.

To understand the staircase-like behavior of the dependence of the emissivity on the amplitude, it is necessary to analyze the different channels that contribute to the modified Urca process. These channels are schematically shown in Fig. 3 and their contribution to the modification function $R_{\tilde{\epsilon}}$ is shown in Fig. 4 where we can already see how gap bridging is manifested at different values of $\hat{\mu}_\Delta$ depending on the channel, so the sum of all the channels yields a staircase dependence on $\hat{\mu}_\Delta$.

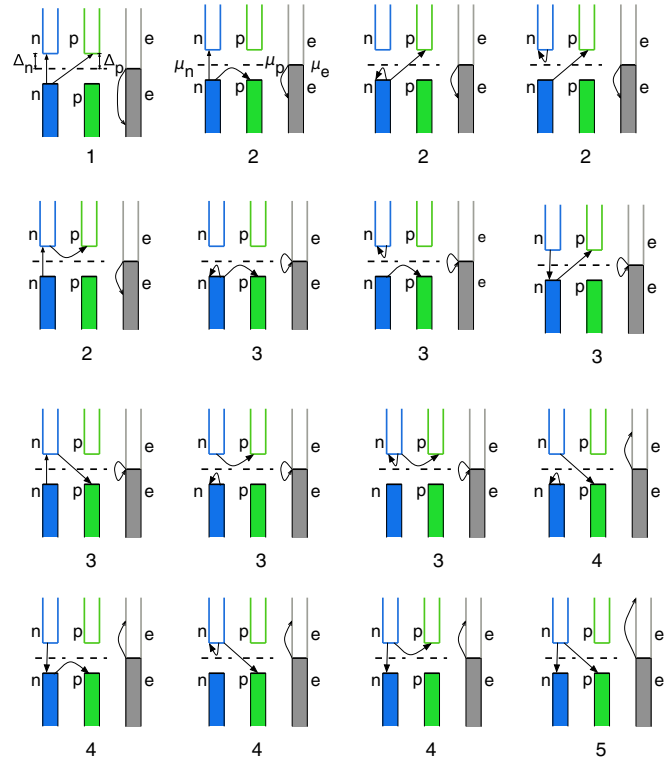

FIG. 3. The 16 channels that contribute to the modified Urca process. For each channel we show the three Fermi seas: from left to right, neutron (gapped), proton (gapped), and electron (ungapped) with their Fermi energies aligned. The black arrows show the transitions of the spectator neutron (leftmost arrow), the $n \leftrightarrow p$ conversion (arrow that goes from neutron to proton Fermi sea) and electron (rightmost arrow). The vertical lengths of the arrows represent the free energy input or output; by energy conservation these add up to zero in each process.

Figure 3 contains 16 panels showing all the channels that contribute to the modified Urca process. Each of the two nucleons can have an initial state above or below its Fermi energy and a final state above or below its Fermi energy, yielding $2^4 = 16$ possibilities. For each channel we show the three Fermi seas in β equilibrium: from left to right, neutron (gapped), proton (gapped), electron (ungapped). We are interested in the free energy $\epsilon_i - \mu_i$ of each species i, so the Fermi energies are aligned. The black arrows show the transitions of the spectator neutron, the $n \leftrightarrow p$ conversion (arrow that goes from neutron to proton Fermi sea), and electron. The vertical length of each arrow shows the free energy input or output, so by energy conservation and β equilibration ($\mu_n = \mu_p + \mu_e$) these add up to zero in each process. The electron line starts at the electron Fermi energy because the free energy cost of placing an electron there is zero. The length of the electron arrow then tells us the amount of energy yielded (or consumed) by the hadronic processes.

A. Rates at zero compression amplitude

The processes fall into five classes, labeled by the number below each panel. At $\hat{\mu}_\Delta = 0$ the degree of suppression of

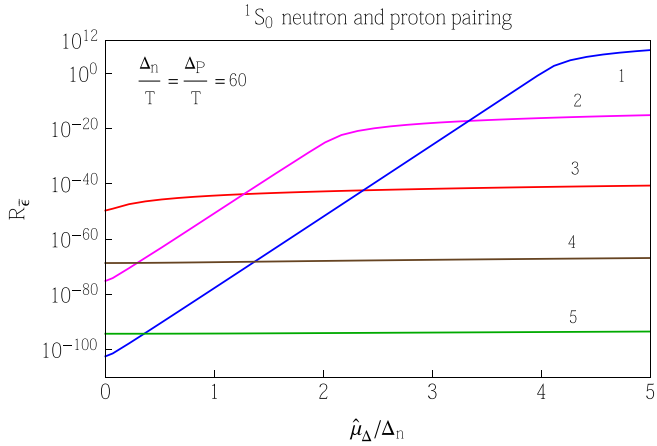

FIG. 4. Amplitude dependence of the neutrino emissivity for different channels that contribute to the modified Urca process. This explains the step structure in Fig. 2.

the rate for each process can be estimated by keeping track of the Boltzmann factors that arise when one tries to annihilate a fermion in a sparsely populated part of phase space, or create a fermion in a densely occupied part of phase space, according to the following rules:

(i) For each arrow starting at energy $+|E|$ (i.e., above the Fermi surface): a factor of $\exp(-|E|/T)$.
(ii) For each arrow ending at energy $-|E|$ (i.e., below the Fermi surface): a factor of $\exp(-|E|/T)$.

The result of applying this rule to each class of channel is

$$\begin{aligned} \text{Classes 1 and 5:} &\quad \exp(-4\Delta/T), \\ \text{Classes 2 and 4:} &\quad \exp(-3\Delta/T), \\ \text{Class 3:} &\quad \exp(-2\Delta/T). \end{aligned} \tag{15}$$

For example, class 1 contains one channel (top left panel of Fig. 3). To see that this has a suppression factor of $\exp(-4\Delta/T)$, we look at each arrow in turn. The spectator neutron transitions from an occupied state at free energy $-\Delta_n$ to an unoccupied state at free energy $+\Delta_n$, so it contributes no suppression factor according to the rules. The "protagonist" neutron starts in an occupied state at free energy $-\Delta_n$ and becomes a proton in an unoccupied state at free energy $+\Delta_p$, so it also contributes no suppression factor. However, these two processes each require an energy input of 2Δ so the electron that is created by the β process must produce 4Δ by ending up in a state at free energy -4Δ which is deep in the occupied electron sea, yielding a suppression factor of $\exp(-4\Delta/T)$ which reflects the unlikeliness of finding an unoccupied state there.

We can now understand the $\hat{\mu}_\Delta = 0$ part of Fig. 4: channels 1 and 5 are the most suppressed, then channels 2 and 4, and finally the least suppressed is channel 3 where the nucleon transitions are energy neutral so the electron yields or requires no energy.

B. Rates as a function of compression amplitude

We now analyze the variation of the rates in the various channels in the presence of a density oscillation whose amplitude $\hat{\mu}_\Delta$ rises to values as large as $5\Delta_n$. The external compression drives the system out of β equilibrium. Under a relatively fast compression the proton and neutron Fermi energies increase by the same fraction, but because the proton fraction in β-equilibrated matter rises with density, the proton Fermi energy is then μ_Δ below its β-equilibrated value at the higher density. This reflects the fact that the system now "wants to make more protons."

The rules are modified as follows:

(i) For channels where the electron is created with energy $-|E|$ (i.e., below the electron Fermi energy), its Boltzmann factor is now $\exp[(-|E| + \mu_\Delta)/T]$, or $(\mu_\Delta/T)^8$ if $\mu_\Delta > E$.
(ii) For channels where the electron is created with energy above the electron Fermi energy, there is an additional overall factor of $(\mu_\Delta/T)^8$ (suprathermal enhancement).

In channels of classes 3–5, at $\hat{\mu}_\Delta = 0$ the electron is created in a state at or above the Fermi energy. There is therefore no gap bridging, just suprathermal enhancement which multiplies the $\hat{\mu}_\Delta = 0$ rate by $(\mu_\Delta/T)^8$. On the log scale used in Fig. 4 this gives a very weak growth with $\hat{\mu}_\Delta$ which appears as the horizontal lines at approximately $\exp(-2\Delta/T)$ (class 3 channels), $\exp(-3\Delta/T)$ (class 4 channels) and $\exp(-4\Delta/T)$ (class 5 channels). For class 3 channels, where the electron is created at its Fermi energy, there is small gap-bridging growth at very small amplitudes where $\mu_\Delta \sim T$.

In class 2 channels, at $\hat{\mu}_\Delta = 0$ the hadronic processes are suppressed in two ways. First, there is a Boltzmann factor of $\exp(-\Delta/T)$ from either trying to place a final-state hadron in the mostly occupied states below the gap, or from finding an initial-state hadron in the sparsely occupied states above the gap. Second, the hadronic processes require an energy input of 2Δ, either to move the spectator neutron up above its pairing gap, or to convert the other neutron into a proton above its pairing gap. This leads to an additional suppression by $\exp(-2\Delta/T)$ since to deliver this amount of energy the electron must be created at free energy -2Δ, deep in its occupied Fermi sea. As $\hat{\mu}_\Delta$ increases, this second factor is canceled by gap bridging: the required energy input is reduced by $\hat{\mu}_\Delta$, since the proton Fermi sea is lowered by this amount. The electron can therefore be created in a state with free energy $\hat{\mu}_\Delta - 2\Delta$, so the second Boltzmann suppression factor is reduced and eventually when $\hat{\mu}_\Delta \approx 2\Delta$ the electron has enough energy to be placed in a state above its Fermi energy where there are plenty of unoccupied states and there is no Boltzmann suppression factor. Any further increase in $\hat{\mu}_\Delta$ only results in suprathermal enhancement, with the remaining $\exp(-\Delta/T)$ (described at the start of this paragraph) which is not affected by gap bridging.

In channel 1, all the hadrons are taken from below the gap and created above the gap, so there are no Boltzmann factors associated with hadronic Fermi-Dirac distributions. However, this requires a large energy input (4Δ at $\hat{\mu}_\Delta = 0$) from the electron, which leads to a suppression factor of $\exp(-4\Delta/T)$ from forcing the electron into the heavily occupied phase space deep in its Fermi sea at a free energy of -4Δ. As $\hat{\mu}_\Delta$ rises, the

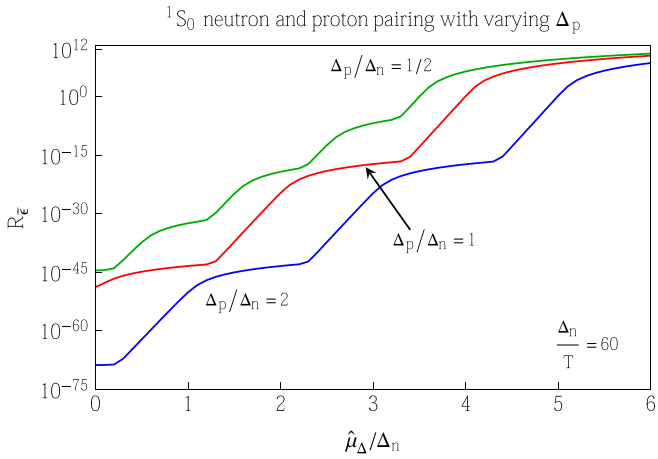

FIG. 5. How the amplitude dependence of the neutrino emissivity depends on the $^1S_0$ proton pairing gap, for $^1S_0$ neutron pairing with $\Delta_n/T = 60$. We show curves for $\Delta_p/\Delta_n = 1/2$, 1, 2.

proton energy states drop relative to the neutron ones, and the $n \to p$ process requires less and less energy. At $\hat{\mu}_\Delta = 2\Delta$ the process breaks even, and at $\hat{\mu}_\Delta = 4\Delta$ it can provide all the energy needed by the spectator neutron. The electron is then relieved of the requirement to subsidize the hadrons, and can be created above its Fermi energy. All Boltzmann suppression has been canceled by gap bridging, and further increase in $\hat{\mu}_\Delta$ produces only suprathermal enhancement. In conclusion, even though this channel is the most suppressed at $\hat{\mu}_\Delta = 0$ it dominates at large $\hat{\mu}_\Delta$ because all the suppression arises from the hadronic energy requirements, which can be eliminated by gap bridging.

Up to now we have assumed that the protons and neutrons have the same pairing gap. We now explore the effect of varying the proton gap: fixing the temperature so that $\Delta_n/T = 60$, we plot the amplitude dependence of the emissivity for $\Delta_p/\Delta_n = 2, 1, 1/2$.

In Fig. 5 we show the results of this variation in Δ_p. Not surprisingly, lower values of the proton gap bring the point of complete gap bridging to a lower $\hat{\mu}_\Delta/\Delta_n$. This is because at large $\hat{\mu}_\Delta/\Delta_n$ the rate is dominated by channel 1 where, as explained in the previous paragraph, all the suppression comes from the energy requirements of the hadronic processes. For the spectator neutron to jump the gap requires $2\Delta_n$ and the conversion of a neutron below the gap to a proton above the gap requires energy $\Delta_n + \Delta_p$, so the total requirement is $3\Delta_n + \Delta_p$. Thus when $\Delta_p/\Delta_n = 1/2$ full gap bridging can be achieved when $\hat{\mu}_\Delta/\Delta_n \approx 3.5$ (top curve in Fig. 5) rather than $4\Delta_n$ when $\Delta_p = \Delta_n$ (middle curve in Fig. 5).

When $\Delta_p/\Delta_n = 2$, the suppression factor is $\exp(-5\Delta_n/T)$ so a compression oscillation of magnitude $\hat{\mu}_\Delta/\Delta_n \approx 5$, is necessary for complete gap bridging.

IV. TRIPLET STATE ($^3P_2$) NEUTRON PAIRING

We now calculate the modified Urca neutrino emissivity for nuclear matter in the inner regions of a neutron star where the neutron density is high and the neutrons pair in a $^3P_2$ channel, while the proton density is relatively low and the protons pair in a $^1S_0$ channel [19]. For the neutrons there are other available triplet channels, but $^3P_0$ is only weakly attractive while the $^3P_1$ state is repulsive [1,20]. For the $^3P_2$ channel, there is still a choice of orientation of the condensate: J_z could be 0, ±1, ±2. Microscopic calculations [19,21,22] find that $J_z = 0$ is very slightly energetically favored over the other values; however this is not conclusive because of uncertainties in the microscopic theory [23]. In the following discussion we will consider neutron condensates with $J_z = 0$ and ±2. We expect these to show different dependencies of the emissivity on temperature and oscillation amplitude because for $J_z = 0$ all neutron states at the Fermi surface are gapped, but for $J_z = \pm2$ there are ungapped nodes at the poles [14].

In our calculations we will assume $\Delta_p = \Delta_n$ for simplicity. In real neutron star core matter it is likely that Δ_p is significantly larger than Δ_n [3].

A. $^3P_2(J_z = 0)$ neutron pairing

For neutrons that Cooper pair in the $^3P_2$ state with $J_z = 0$, rotational symmetry is broken. There is a preferred direction in space (we will align the z axis along it) and the gap in the neutron spectrum becomes dependent on the angle θ between the momentum of the neutron quasiparticle and the z axis [19],

$$\Delta_n(\theta) = \Delta_{n0}\sqrt{1 + 3\,\cos^2(\theta)}. \tag{16}$$

Note that the gap varies between a minimum of Δ_{n0} (around the equator) and $2\Delta_{n0}$ (at the poles) but does not vanish anywhere on the Fermi surface. We therefore expect that $^3P_2$ pairing will be qualitatively similar to $^1S_0$ pairing, having the same parametric dependence of the rate on temperature and oscillation amplitude.

The dependence of the $^3P_2$ gap on θ restricts us from separating the angular and radial part of the integral in Eq. (5). However, the gap has no ϕ dependence so we can integrate the momentum-conserving δ function in Eq. (5) over the azimuthal angles analytically [24]

$$\int_0^{2\pi} d\phi_1\, d\phi_2\, d\phi_3\, \delta^3(P_1 + P_2 + P_3) = \frac{4\pi\,\Theta\left(\frac{3}{4} - c_1c_2 - c_1^2 - c_2^2\right)}{p_{Fn}^3\sqrt{\frac{3}{4} - c_1c_2 - c_1^2 - c_2^2}}\delta(c_1 + c_2 + c_3), \tag{17}$$

where $c_j \equiv \cos\theta_j$ and Θ is the unit step function. We then perform the remaining angular and radial integrals numerically.

Figure 6 shows how the neutrino emissivity is affected by increasing the amplitude of compression oscillations. Since the neutrons are gapped everywhere on the Fermi surface we expect the results to be similar to those calculated for $^1S_0$ neutron pairing in Sec. III, and comparing Fig. 6 with Fig. 2 we see this this is indeed the case. The overall pattern of the dependence on T and $\hat{\mu}_\Delta$ is the same, the only difference is that $R_{\tilde{\epsilon}}$ for $^3P_2(J_z = 0)$ pairing is smaller than for $^1S_0$ pairing by a factor that varies between 400 and 20 as $\hat{\mu}_\Delta$ ranges from 0 to $5\Delta_n$.

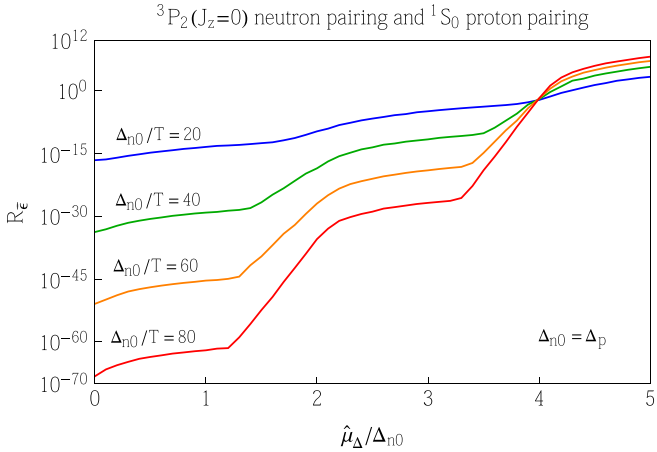

FIG. 6. Dependence of the neutrino emissivity on the amplitude of the applied compression oscillations, for $^3P_2$ ($J_z = 0$) neutron pairing and $^1S_0$ proton pairing.

B. $^3P_2(J_z = \pm 2)$ neutron pairing

We now consider the case where the neutron Cooper pairs are in the $^3P_2$ state with $|J_z| = 2$ while the protons pair in the $^1S_0$ channel. The angular dependence of the neutron gap in this channel is [19]

$$\Delta_n(\theta) = \Delta_{n0} \sin(\theta). \tag{18}$$

Note that the neutron gap vanishes at the poles and has a maximum value of Δ_{n0} around the equator.

In Fig. 7, we show the effect of increasing the amplitude of the applied compression oscillations. To explain this figure we first explain how the angular dependence of the gap affects the modified Urca process. In Fig. 8 we have plotted a typical arrangement of the neutron momenta. To understand the overall behavior we can neglect the proton and electron Fermi momenta, which are significantly smaller than the neutron Fermi momentum. The momenta of the incoming neutrons n_1 and n_2 (Fig. 1) then add up to the momentum of the

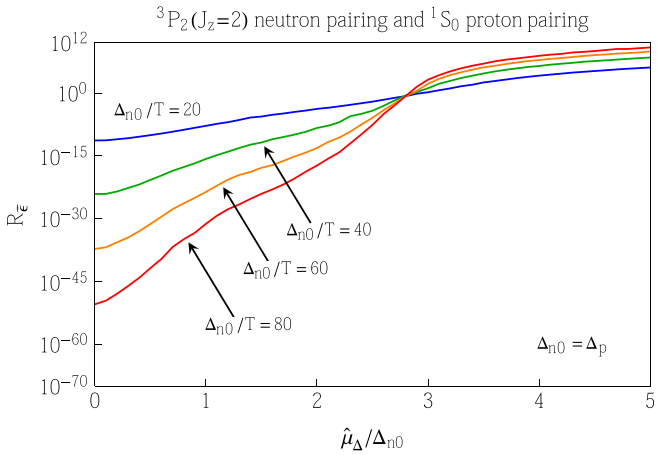

FIG. 7. Dependence of neutrino emissivity on the amplitude of the applied compression oscillations for $^3P_2$ ($J_z = 2$) neutron pairing and $^1S_0$ proton pairing.

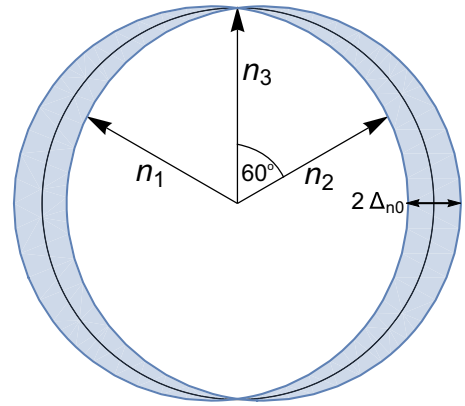

FIG. 8. Momenta of the neutrons in one example of a typical Urca process in a $^3P_s(J_z = \pm 2)$ neutron superfluid. The shaded region is the gap at the neutron Fermi surface. The momenta of the two initial-state neutrons n_1 and n_2 add up to the momentum of the final-state neutron n_3 (neglecting the proton and electron momenta). Only one of the three neutron momenta can be at a gapless node on the Fermi surface.

outgoing neutron n_3. Since all three neutron momenta lie near the neutron Fermi surface, p_{n1} and p_{n2} must be at a 60° angle to p_{n3}, on opposite sides in the same plane. Only one of the three neutrons can be at the gapless node on their Fermi surface. In Fig. 8 we placed p_{n3} at the node. The other two neutron momenta are at $\theta = \pi/3$ where the gap is $\sqrt{3}\Delta_{n0}/2$.

We can now understand the effect of increasing the amplitude of the applied compression oscillations, as shown in Fig. 7. For low amplitudes the neutrino emissivity is exponentially suppressed by the gap, roughly as $\exp(-1.73\Delta_{n0}/T)$, as compared with $\exp(-2\Delta_n/T)$ for $^1S_0$ neutron pairing (Fig. 2). It is natural to expect the $^3P_2(J_z = \pm 2)$ pairing to be less suppressed because there is a gapless node on the neutron Fermi surface.

To understand more fully the origin of the suppression factor, we analyze one of the dominant channels at low $\hat{\mu}_\Delta/\Delta_{n0}$, shown in Fig. 9(a). In the figure we show two neutron Fermi seas, one gapless, corresponding to a neutron momentum at the gapless node on the Fermi surface (polar angle $\theta = 0$), and one with a gap of $\sqrt{3}\Delta_{n0}/2 \approx 0.866\Delta_{n0}$, corresponding to neutron momenta at $\theta = \pi/3$ or $2\pi/3$. For the process shown in Fig. 9(a) there is a suppression factor of $\exp(-\sqrt{3}\Delta_{n0}/t) \approx \exp(-1.73\Delta_{n0}/t)$, arising from the unlikelihood of finding both initial-state neutrons in the sparsely occupied region above the gap at $\theta = \pi/3$. The final-state neutron is at the gapless node and so experiences no Boltzmann suppression. The electron is created above its Fermi surface (because the hadrons provide an energy surplus to be absorbed by the electron) so it too experiences no Boltzmann suppression.

As we see in Fig. 7, increasing the amplitude of compression oscillation leads to gap bridging: some of the β processes become unsuppressed which results in steady increase of the neutrino emissivity until at $\hat{\mu}_\Delta/\Delta_{n0} \approx 2.73$ the β process rate reaches the ungapped limit ($R_\epsilon \sim 1$), regardless of how low the temperature may be.

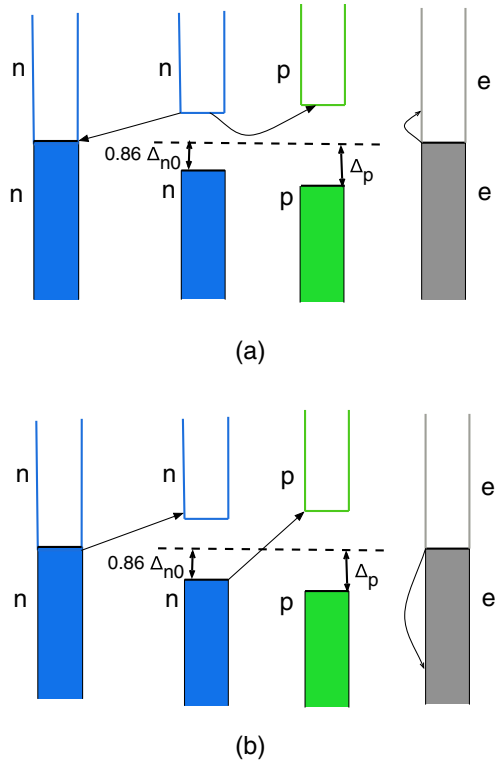

FIG. 9. Channels that in the presence of ${}^3P_2(J_z = \pm 2)$ neutron pairing and ${}^1S_0$ proton pairing will dominate the modified Urca process in different regimes: (a) at low μ_Δ/Δ_{n0}, (b) at high μ_Δ/Δ_{n0}.

To understand why complete gap bridging happens at $\hat{\mu}_\Delta/\Delta_{n0} \approx 2.73$, we show in Fig. 9(b) the channel of class 1 (Fig. 3) which dominates at large $\hat{\mu}_\Delta/\Delta_{n0}$. As in the case of ${}^1S_0$ neutron pairing, this is because all the suppression comes from the energy requirements of the hadronic sector, none from hadronic Fermi-Dirac factors (all hadrons start below the gap and end in the sparsely occupied region above the gap). At $\hat{\mu}_\Delta = 0$ the energy required for this is $0.866\Delta_{n0}$ for $n_1 \to n_3$ and $0.866\Delta_{n0} + \Delta_p$ for $n_2 \to p$, totalling $2.73\Delta_{n0}$ assuming $\Delta_p = \Delta_{n0}$. This energy is supplied by the electron, which must be created deep in its Fermi sea at a free energy of $-2.73\Delta_{n0}$, yielding a Boltzmann suppression of $\exp(-2.73\Delta_{n0}/T)$.

As we increase $\hat{\mu}_\Delta$, the proton Fermi surface is lowered by $\hat{\mu}_\Delta$ relative to the neutron Fermi surface and the $n \to p$ process requires less and less energy. At $\hat{\mu}_\Delta = 1.866\Delta_{n0}$ the $n \to p$ process breaks even, and at $\hat{\mu}_\Delta = 2.73\Delta_{n0}$ it can provide all the energy needed by the spectator neutron. The electron can then be created above its Fermi energy. All Boltzmann suppression has then been canceled by gap bridging, and further increase in μ_Δ produces only suprathermal enhancement.

V. CONCLUSION AND DISCUSSION

We have shown that the exponential suppression of flavor-changing β processes in superfluid and superconducting nuclear matter can be completely overcome, via the mechanism of gap bridging, by compression oscillations of sufficiently high amplitude, regardless of how low the temperature may be. This confirms the conjecture outlined in previous work [5], and shows that it applies to the realistic case of modified Urca processes and ${}^3P_2$ neutron pairing.

We expect gap bridging to be relevant in processes that induce density oscillations of amplitude $\Delta n/\bar{n} \sim 10^{-3}$ to 10^{-2} [5]. This is sufficient to overcome typical nucleon pairing gaps which are of order 1 MeV. In hyperonic [25,26] or quark [27,28] matter, there are processes which are only suppressed by $\Delta \lesssim 0.01$ MeV, and these could be bridged by oscillations with amplitudes as small as $\Delta n/\bar{n} \lesssim 10^{-4}$. Relevant physical scenarios that are likely to involve high-amplitude oscillations include unstable oscillations of rotating compact stars such as f-modes or r-modes [10], events like star quakes [12], and neutron star mergers [13]. When such high-amplitude compression oscillations occur in superfluid or superconducting matter, certain transport properties, such as bulk viscosity and neutrino emissivity, will be greatly enhanced, leading to nonlinear (in amplitude) damping of the mode itself, and enhanced cooling via neutrino emission.

ACKNOWLEDGMENTS

We thank Kai Schwenzer for valuable comments. This material is based upon work supported by the U.S. Department of Energy, Office of Science, Office of Nuclear Physics under Award No. DE-FG02-05ER41375.

[1] D. Dean and M. Hjorth-Jensen, Rev. Mod. Phys. **75**, 607 (2003).
[2] H. Müther and W. H. Dickhoff, Phys. Rev. C **72**, 054313 (2005).
[3] D. Ding, A. Rios, H. Dussan, W. H. Dickhoff, S. J. Witte, A. Carbone, and A. Polls, Phys. Rev. C **94**, 025802 (2016).
[4] J. M. Lattimer and M. Prakash, Science **304**, 536 (2004).
[5] M. G. Alford, S. Reddy, and K. Schwenzer, Phys. Rev. Lett. **108**, 111102 (2012).
[6] J. Madsen, Phys. Rev. D **46**, 3290 (1992).
[7] A. Reisenegger, Astrophys. J. **442**, 749 (1995).
[8] M. G. Alford, S. Mahmoodifar, and K. Schwenzer, J. Phys. G **37**, 125202 (2010).
[9] M. E. Gusakov and E. M. Kantor, Mon. Not. Roy. Astron. Soc. **428**, L26 (2013).
[10] N. Stergioulas, Living Rev. Relativity **6**, 3 (2003).
[11] M. G. Alford and K. Schwenzer, Astrophys. J. **781**, 26 (2014).
[12] L. M. Franco, B. Link, and R. I. Epstein, Astrophys. J. **543**, 987 (2000).
[13] D. Tsang, J. S. Read, T. Hinderer, A. L. Piro, and R. Bondarescu, Phys. Rev. Lett. **108**, 011102 (2012).
[14] D. Yakovlev, A. Kaminker, O. Y. Gnedin, and P. Haensel, Phys. Rep. **354**, 1 (2001).
[15] A. Sedrakian, Phys. Lett. B **607**, 27 (2005).
[16] A. Sedrakian, Prog. Part. Nucl. Phys. **58**, 168 (2007).

[17] B. Friman and O. Maxwell, Astrophys. J. **232**, 541 (1979).
[18] D. G. Yakovlev and K. P. Levenfish, Astron. Astrophys. **297**, 717 (1995).
[19] T. Takatsuka and R. Tamagaki, Prog. Theor. Phys. **46**, 114 (1971).
[20] R. Tamagaki, Prog. Theor. Phys. **44**, 905 (1970).
[21] M. Baldo, J. Cugnon, A. Lejeune, and U. Lombardo, Nucl. Phys. A **536**, 349 (1992).
[22] L. Amundsen and E. Østgaard, Nucl. Phys. A **442**, 163 (1985).
[23] A. Y. Potekhin, J. A. Pons, and D. Page, Space Sci. Rev. **191**, 239 (2015).
[24] M. Gusakov, Astron. Astrophys. **389**, 702 (2002).
[25] M. Prakash, M. Prakash, J. M. Lattimer, and C. J. Pethick, Astrophys. J. Lett. **390**, L77 (1992).
[26] P. Haensel, K. P. Levenfish, and D. G. Yakovlev, Astron. Astrophys. **381**, 1080 (2002).
[27] A. Schmitt, I. A. Shovkovy, and Q. Wang, Phys. Rev. D **73**, 034012 (2006).
[28] X. Wang and I. A. Shovkovy, Phys. Rev. D **82**, 085007 (2010).